Soft Matter

Accepted Manuscript

ROYAL SOCIETY OF CHEMISTRY

www.rsc.org/softmatter

A table of contents entry

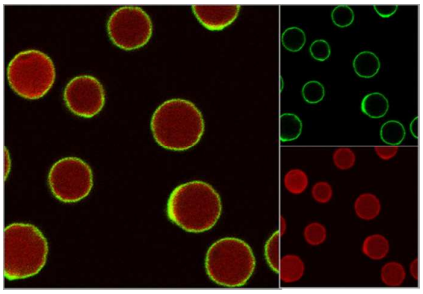

Hydrogen-bonded multilayers of tannic acid can be used for highly efficient doxorubicin encapsulation and storage in the pH range 5<pH<7.5.

Encapsulation of anticancer drug by hydrogen-bonded multilayers of tannic acid

*Fei Liu,[1] ‡ Veronika Kozlovskaya,[1] ‡ Oleksandra Zavgorodnya,[1] Claudia Martinez-Lopez,[1] Shane Catledge,[2,3] and Eugenia Kharlampieva[1,3]**

[1]Department of Chemistry,[2] Department of Physics, University of Alabama at Birmingham, Birmingham, AL, 35294, USA
[3]Center for Nanoscale Materials and Biointegration, University of Alabama at Birmingham, Birmingham, AL, 35294, USA

*Correspondence address: 901 14th St South, CHEM294, Birmingham, AL, USA, 35294, e-mail: ekharlam@uab.edu

‡The authors equally contributed to this work

KEYWORDS:

Tannic acid, poly(N-vinylpyrrolidone), hydrogen-bond assembly, doxorubicin encapsulation, pH-sensitive, salt-dependent permeability

Abstract

Tannic acid (TA)-based multilayer assemblies have attracted increasing interest for biomedical applications. Here we explore properties of TA/poly(N-vinylpyrrolidone) (TA/PVPON) hydrogen-bonded multilayers for drug encapsulation and long-term storage. We demonstrate that the small molecular weight anticancer drug, doxorubicin (DOX), can be successfully loaded into (TA/PVPON) capsules with high encapsulation efficiency. We have also found that the encapsulated DOX can be efficiently stored inside the capsules for the pH range from pH=7.4 to pH=5. We show that the chemical and functional stability of TA at neutral and basic pH values is achieved through complexation with PVPON. The UV-vis spectrophotometry and *in situ* ellipsometry analyses of the hydrogen-bonding interactions between TA and PVPON at different pH values reveal pH-dependent behavior of TA/PVPON capsules for the pH range from pH=7.4 to pH=5. Increasing deposition pH value from pH=5 to pH=7.4 leads to a 2-fold decrease in capsule thickness. However, this trend is reversed when salt concentration of the deposition solutions is increased from 0.01 M to 0.1 M NaCl. We have also demonstrated that the permeability of (TA/PVPON) capsules prepared using low salt deposition conditions and pH=7.4 can be increased 2-fold by exposure of the capsules to 0.1 M NaCl salt solutions at the same pH. Our work opens new perspective for design of novel polymer carriers for controlled drug delivery in cancer therapy.

Introduction

The use of hollow particulates is considered a powerful tool in drug delivery.[1,2] However, many therapeutics and small molecular weight drugs in particular are activated intracellularly, which poses a challenge for their intravenous application. This is due to low solubility of those drugs in an aqueous environment, high toxicity, rapid clearance and, consequently, a need for their delivery to specific intracellular points. Polymeric encapsulation has been shown suitable for solubilizing these drugs by shielding their surfaces with water-soluble macromolecules which could be simultaneously functionalized for specific targeting.[3,4]

Various delivery approaches have been investigated, making use of continuous polymeric particles, micelles, and other polymer-drug constructs.[5,6,7,8] Hollow polymeric particles, known as capsules, have been made using the layer-by-layer (LbL) technique.[9,10] This involves a sequential assembly of polymers onto sacrificial substrates followed by substrate dissolution and has attracted considerable interest because of the high payloads and controlled release of the therapeutics.[11,12,13] The multilayer capsules comprise ultrathin multilayer shells (<50 nm) and sub- or micrometer size cavities used for loading and delivery of functional cargo.[14] Unlike other hollow polymer particles, chemical, mechanical, and surface properties of the LbL capsules can be precisely tailored by choosing appropriate polymers, deposition conditions, and the nature of sacrificial templates.[9] The LbL shell can be further functionalized for a specific biological response.[15]

Tannic acid (TA)-based assemblies have recently attracted extensive research attention due to diverse biological properties of TA including antioxidant and anticarcinogenic[16,17,18] and its capability of interaction with proteins,[19] which have been explored for biomedical applications.[20,21,22,23,24] TA belongs to a group of hydrolysable tannins and contains digalloyl ester groups connected to a glucose core which has been shown to be versatile for a variety of industrial[25,26] and food applications.[27,28] The chemical structure of TA rich in phenolic groups has allowed interactions based on ionic pairing,[12b] hydrogen bonding,[29,30] and metal coordination.[31] Lvov *at al.* reported ionically-paired multilayers of TA with poly(dimethyldiallyl ammonium chloride) and poly(allylamine hydrochloride) (PAH) polycations, thereby demonstrating varied pH-dependent permeability.[12b] Erel-Unal and Sukhishvili found that pH-stability of hydrogen-bonding multilayers of TA correlated with the

phase behavior of TA complexes in solution.[29a] Complexation between TA and methylcellulose has recently been studied by Velikov *et al*. who showed that methylcellulose interfacial stiffness was enhanced by the complexation.[32] The binding stoichiometry indicated that 33 molecules of TA were bonded to methylcellulose via hydrogen bonding. Later, Khutoryanskiy *et al*. demonstrated that the interfacial hydrogen bonding between methylcellulose and TA can be used to produce hollow capsules with the size of hundreds of microns loaded with model drugs.[33] They demonstrated that the hollow TA/methylcellulose capsules exhibited better pH-stability compared to poly(acrylic acid) (PAA)/ methylcellulose capsules.[33] The ability of TA to form complexes with the antihistaminic drug BromPheniramine Maleate in phosphate buffer at pH=6.8 was also explored to produce formulations with sustained drug release.[34] Hammond *et al.* developed pH-controlled drug releasing films and hemostatic coatings from hydrogen-bonded TA multilayers.[35,36] Sukhishvili and co-workers have recently assembled thermoresponsive PVPON-*b*-poly(N-isopropylacrylamide) block copolymer micelles into multilayers using TA as a physical cross-linker of the micelle layers.[37] The micelle films swelled upon temperature increase and released an anti-cancer drug.[37,38] An improvement in the antioxidant stability of a drug formulation was reported by He *et al*. when poly(triethylene glycol methyl acrylate-co-tocopheryl acrylate) complexed with TA was used as a potential antioxidant prodrug to enable localized neuro-protection. The prodrug was demonstrated to possess an enhanced endurance to the oxidative stress that was induced by the presence of hydrogen peroxide.[39] Recently, Caruso and co-workers assembled metal-TA complexed films and capsules based on metal-ligand coordination.[40]

Despite the demonstrated versatility and unique applications of TA-based systems, little is known about how chemical and physical properties of TA hydrogen-bonded multilayer films and capsules can be controlled by varying fabrication conditions. Our group recently demonstrated that (TA/PVPON) multilayer coatings prolonged viability and function of pancreatic islets, while (TA/PVPON) capsules showed immunomodulatory properties by suppressing immune cell-mediated proinflammatory cytokine synthesis.[20] We also produced cubic, spherical, and hemispherical TA/PVPON microcapsules capable of maintaining their shapes in a dry state as controlled by capsule wall rigidity.[21] The hemispheres were internalized by macrophages two-fold more efficiently than the spherical capsules.

In the current work, we explore properties of (TA/PVPON) hydrogen-bonded multilayers for drug encapsulation, long-term storage, and release. We investigate the effects of pH and salt concentration on chemical stability and complexation of TA with PVPON in solution and within multilayers. Physicochemical properties of multilayer films and capsules including thickness, permeability, and encapsulation and pH-triggered release of the anticancer drug doxorubicin (DOX) in/from capsule interiors are studied under various pH and salt conditions. To the best of our knowledge this is the only example of applying hydrogen-bonded multilayer capsules for loading and pH-triggered delivery of anticancer drugs.

Results and Discussion

Prior to DOX encapsulation, the effects of solution pH and ionic strength on assembly and properties of hydrogen-bonded TA complexes and multilayers were studied. Since TA is capable of scavenging free radicals due to its rich phenolic component,[41] understanding chemical stability of TA is crucial for controlling properties of hydrogen-bonded multilayer films and capsules.

Stability of TA in hydrogen-bonded complexes in solutions under varied pH. Stability of TA in solution and in TA/PVPON complexes was explored in the pH range from 2 to 9 in the presence of 0.15 M NaCl. As shown in Figure 1a, the solutions of TA freshly prepared at the pH values in the range from pH=2 to pH=5 have a strong absorption peak at a wavelength of 276 nm corresponding to non-ionized phenolic groups. However, when the pH is increased further to pH=6, a new absorption band at ~325 nm appears and its intensity increases steadily with pH up to pH=9. In this pH region, titration of the phenolic groups on TA occurs leading to a fully ionized structure at pH=9. Thus, the ratio of the TA solution absorbance peak at 276 nm to that at 321 nm (A276/A321) can be used to monitor the ionization of TA in solution (Fig. 1b). As the amount of the ionized phenolate groups increases, the A276/A321 ratio decreases with approximately 50% ionization of TA occurring at pH=6 (Inset in Fig. 1b). This result falls in the range of 5 to 8.5 previously found for pK_a values of TA.[42] To explore pH-triggered stability of TA, the absorbance of protonated (pH=5) and deprotonated (pH=7.4) 0.5 mg mL^{-1} solutions of TA was monitored for 24 h using the solutions sealed and kept in the dark before the measurements. We found that the TA solutions at lower pH values in the range from pH=2 to

pH=5 were chemically stable, exhibiting the main absorbance peak at 276 nm after 24 h of the solution preparation (Fig. 1c). The UV-vis spectroscopy of the TA solutions prepared at high pH values, however, revealed some chemical changes in the TA solution at pH=7.4. This was manifested after 1 hour of solution preparation by the appearance of strong absorbance bands at 255 nm and at 370 nm, and by blue-shifting the initial absorption band at 276 nm to a stronger absorption band at 270 nm (Fig. 1d). Instability of TA at pH> 7 was previously found by Erel-Unal et al and was attributed to oxidation by atmospheric oxygen under light.[29a] We found that de-oxygenation, sealing, and storing the solutions in the dark does not prevent structural re-arrangements of TA at pH=7.4. Thus, the observed absorbance changes are most likely due to rearrangements of an ionized structure of TA at high pH to various conjugated quinone derivatives.[43] In our experiments all TA solutions at pH > 5 used in the studies of hydrogen-bonded assemblies of TA/PVPON were freshly prepared and used within 1 hour of preparation.

Next, we studied the chemical stability of TA within its hydrogen-bonded complexes with PVPON which were formed at pH=5 and at pH=7.4. Under these conditions, 0.5 mg mL^{-1} TA solution at the appropriate pH value was mixed with 1 mg mL^{-1} PVPON solution at the same pH to produce the water non-soluble hydrogen-bonded complex, TA/PVPON. The formed precipitate was collected by centrifugation and washed with the corresponding buffer to remove unbound TA and PVPON from the TA/PVPON complex. The TA/PVPON precipitate was re-dispersed in the appropriate pH buffer solution, and its UV-vis spectrum was monitored for 24 h. Chemical changes of TA within the hydrogen-bonded complex were directly monitored between 250 nm and 500 nm since PVPON solutions are transparent in this region (Figure S1). Figure 2a demonstrates that the absorbance from the TA complexed with PVPON at pH=5 (0.15 M NaCl) is shifted to lower energy (284 nm compared to 276 nm for free TA in solution at the same pH. This result agrees with the previous UV-vis studies on the position of the phenol group absorption bands in protic and aprotic media which demonstrated the sensitivity of that position to the phenol group state of protonation as well as indicated a correlation between the electronic absorption frequencies of phenolic groups and their hydrogen-bonded states. [44] When the TA/PVPON complex was transferred to pH=7.4, the absorbance shoulder at 325-350 nm appeared, revealing a partial ionization of TA within the TA/PVPON complex (Fig. 1a). However, in contrast to free TA in solution at pH=7.4, TA within the complex remained chemically stable for at least 24 h without showing any sign of structural change observed for

TA in solution at pH=7.4 (Fig. 2a and 1d). Similar stabilization of TA for at least 24 h within the TA/PVPON complex was observed for the TA/PVPON initially formed at pH=7.4 (Fig. 2b). The TA absorbance within the TA/PVPON in the range of 325-350 nm was less intense than that for free TA in solution at pH=7.4, which implies a lower degree of TA ionization within the TA/PVPON at similar pH. This is in agreement with previous studies on hydrogen-bonded polycarboxylic acids that reported the suppressed ionization of the polyelectrolytes due to their hydrogen bonding interactions compared to that for free polyelectrolyte molecules in solution.[45] The uncomplexed phenolic groups present in the TA/PVPON complex formed at pH = 7.4 could be protonated when the TA/PVPON complex was transferred to lower pH = 5. As shown in Figure 2b, the TA absorbance peak at 325-350 nm disappears when the TA/PVPON complex is transferred to pH = 5 and only the absorbance at 284 nm characteristic for the protonated –OH groups of TA (present in the case of TA/PVPON formed at pH=5) is observed in the TA/PVPON spectrum. Also, the suppression of TA ionization within the TA/PVPON is clearly evident from the comparison of absorbance ratios of the protonated/deprotonated TA for free TA solutions with that of the TA/PVPON complex prepared at various pH values (Fig. 2c). It is observed that the apparent pK_a of TA (~50% ionization degree) within the TA/PVPON is shifted to pH ~ 7.4. This is compared to pH ~ 6 for free TA solutions (Fig. 2c).

Our aforementioned results reveal that PVPON stabilizes TA against chemical changes at pH > 7. Although TA ionization is suppressed by interaction with PVPON, it remains pH sensitive. Bound to PVPON, TA can still be reversibly ionized by varying solution pH. In this case, the degree of TA ionization is similar to that for the complex formed at the particular pH value (Fig. 2c). Unlike free TA solutions, the induced TA ionization within the TA/PVPON does not compromise the chemical stability of TA.

Effect of pH and ionic strength on growth of TA/PVPON multilayers. We explored the effect of TA ionization on assembly and other properties (including thickness and morphology) of the TA/PVPON coatings. The growth of the planar TA/PVPON multilayers was investigated at pH = 5 and at pH = 7.4 when TA is in its protonated and deprotonated forms, respectively. To prevent possible roughening of the hydrogen-bonded multilayers induced by drying, which would result in the thickness increase, the multilayer deposition was performed inside the liquid cell and monitored using *in situ* ellipsometry. Figure 3a demonstrates that at low ionic strength

of 0.01 M the multilayers grew linearly at both pH values with the higher average bilayer thickness at the lower pH resulting in 4.2 nm and 1.3 nm for pH = 5 (0.01 M) and pH = 7.4 (0.01 M), respectively. This result agrees with previous studies on hydrogen-bonded LbL films involving ionizable polycarboxylic acids when the increased ionization of the polyacid led to thinner films.[45,46] In contrast, the deposition of the TA/PVPON multilayers at higher ionic strength of 0.1 M reversed the thickness trend and resulted in 3-fold thicker coatings at pH = 7.4 with the average bilayer thickness of 4.6 nm. In the presence of salt, the deposition of the TA/PVPON multilayer at pH = 5 yielded thinner films than that at a lower ionic strength (Fig. 3a). The thicker multilayers at high pH value in the presence of high salt concentration can be obtained due to screening of the negatively charged TA under these conditions. Thus, for example, the PAH or poly(L-lysine) (PLL) multilayers obtained via glutaraldehyde-assisted cross-linking could be produced only in the presence of 0.1 M NaCl. This facilitated the proximity of the similarly charged polyelectrolyte chains when no oppositely charged counterpart was used.[47,48] The lower thickness of the TA/PVPON films obtained at pH=5 in the presence of 0.1 M NaCl can be explained by the salt-induced ionization of TA which could result in mutual repulsion of the neighboring layers of TA leading to the slightly thinner coating than that under low salt conditions of 0.01 M. This result agrees well with the previously found enhanced dissociation of PAA in the presence of high salt concentration which greatly increased the erosion of the hydrogen-bonded PAA/PVPON films for increased pH and salt concentration.[49] It is important to note that during the multilayer deposition, both in low and high salt solutions, some amount of TA that adsorbed on the preceding PVPON layer is removed during the following PVPON layer adsorption. This implies the existence of TA-TA weakly-interacted molecules that are replaced by TA-PVPON competitive interactions (Fig. 3b).

Effect of pH and ionic strength on permeability properties of (TA/PVPON) capsules. We explored the (TA/PVPON) coating thickness dependence on pH and ionic strength using porous particulate templates. Hydrogen-bonded assembly of the TA/PVPON was performed on surfaces of 5 μm porous silica particles. Porous silica was selected due to its capability for loading the porous interiors of the particles with functional molecules, such as therapeutics or imaging species.[50,51,52] Once the desired coatings were formed, the porous silica cores were dissolved in solution of hydrofluoric acid and ammonium fluoride and the obtained hollow capsules were purified by dialysis (see Experimental section for details). AFM analysis of the capsule

morphology shown in Figure 5 revealed that the $(TA/PVPON)_8$ capsules prepared at pH=5 displayed increased surface roughening when ionic strength of the polymer solutions was increased from 0.01 M (Fig. 4a) to 0.1 M (Fig. 4b). In contrast, the opposite effect was observed for the capsules prepared at pH= 7.4. The capsules prepared at low 0.01 M ionic strength (Fig. 4c) exhibited rougher surfaces compared to those produced from high ionic strength solutions of 0.1 M (Fig. 4d). The grainy capsule morphology is correlated to the decrease in the capsule wall thickness. The single wall capsule thickness was measured using AFM (Fig. 4e) and was in agreement with the thickness data obtained on planar films using *in situ* ellipsometry discussed above. Thus, for example, the capsule wall thickness for $PEI(TA/PVPON)_8$ prepared at pH=5 decreased from 60 ± 12 nm to 42 ± 9 nm when the ionic strength of deposition solutions was increased from 0.01 M to 0.1 M (Fig. 5e). Similar to the thickness trend observed for planar TA/PVPON coatings, the thickness of $PEI(TA/PVPON)_8$ capsules prepared at high pH=7.4 increased from 33 ± 10 nm to 65 ± 9 nm when the ionic strength was increased (Fig. 4e). Based on our AFM data, we suggest that the roughened grain morphology of the (TA/PVPON) coatings is observed when TA molecules carry unscreened or induced negative charges. In this case, the repulsion between TA molecules within the multilayer results in rough surfaces of TA/PVPON coatings.

To explore the effect of deposition conditions on permeability properties of TA/PVPON coating, we performed the Fluorescence Recovery After Photobleaching (FRAP) experiments using confocal microscopy and fluorescein isothiocyanate (FITC) as a fluorescent probe.[53,54] The (TA/PVPON) capsules were mixed with FITC solution at pH=5 or pH=7.4 (0.01 M or 0.1 M NaCl). A whole region of the capsule interior was photo-bleached with a laser beam (see Experimental section for details). The fluorescence recovery in that region was monitored with time under the lower laser intensity. The recovery curve was fitted as $I=I_0(1-e^{-At})$, where I and I_0 were the equilibrium and initial fluorescence intensities, respectively.[54,55] The coefficient A was deduced from curve fitting, and the diffusion coefficient of FITC through the capsule wall, D, was obtained as $A=3D/rh$, where r was the capsule radius measured using confocal microscopy, and h was its single wall thickness measured with AFM. Figure 5a shows that FITC permeation inside $PEI(TA/PVPON)_6$ capsules made at pH = 5 at low and high ionic strength were similar, with D = (1.8 ± 0.3) 10^{-11} cm^2 s^{-1} at 0.01 M and (2.5 ± 0.5) 10^{-11} cm^2 s^{-1} at 0.1 M NaCl, respectively. The slightly lower diffusion of FITC through $PEI(TA/PVPON)_6$ capsules was

observed for those prepared at pH = 7.4 and low ionic strength of 0.01 M (D = (1.45 ± 0.27) 10^{-11} cm^2 s^{-1}) compared to that prepared at pH = 5. However, in contrast to pH = 5, the dye permeation drastically increased almost 4-fold when those capsules were prepared at pH = 7.4 and at high ionic strength of 0.1 M (Fig. 5a), resulting in D = (5.8±1.0) 10^{-11} cm^2 s^{-1}. The obtained results can be better understood by taking into consideration the interactions between the dye and the capsule wall at the studied conditions. FITC, an anionic dye, has a pK_a ~ 6.5[56] and is uncharged at pH = 5 (0.01 M). The (TA/PVPON) capsules having more than 90% phenolic groups in TA neutral under these conditions are also uncharged (Fig. 1b and 2c). At a higher ionic strength of 0.1 M, a slight ionization of TA would not lead to significant changes in (TA/PVPON) and the diffusion of FITC will remain similar to that for the capsules prepared at pH = 5 and 0.01 M NaCl. However, the interaction between FITC and the (TA/PVPON) capsule wall is different for the capsules prepared at pH = 7.4. At low ionic strength, both FITC and the (TA/PVPON) capsule wall become anionic, which may cause a mutual repulsion between the dye and the capsule wall. As a result, FITC diffusion is even lower than that at pH = 5 (0.01 M). However, in the presence of 0.1 M NaCl, negative charges are screened and FITC can permeate freely through the capsule wall leading to the 4-fold increase in the FITC diffusion coefficient under these conditions.

We also found that the decrease in pH at high ionic strength led to changes in the capsule wall structure, resulting in the decrease of FITC permeation through the capsule wall. For example, D_{FITC} through PEI(TA/PVPON)$_6$ capsules prepared at pH = 7.4 (0.1 M) decreased almost 2-fold from (5.8±1.0) 10^{-11} cm^2 s^{-1} to (3.9±1.0) 10^{-11} cm^2 s^{-1} when the solution pH was changed to pH = 5 (0.1 M) (Fig. 5b). This result suggests that the capsule wall mesh was decreased due to protonation of TA and formation of additional hydrogen bonds with PVPON. However, this treatment could not completely restore the low permeability of the capsule wall exhibited by the PEI(TA/PVPON)$_6$ capsules that were originally prepared at low pH=5 (0.1 M) (Fig. 5a and b) and had twice lower diffusion D_{FITC} = (2.5 ± 0.5) 10^{-11} cm^2 s^{-1} (Fig. 5a). Similar results were observed for 8-bilayer capsules of (TA/PVPON) (Fig. 5b). Apparently, the high permeability of the TA/PVPON capsules prepared at pH = 7.4 using high salt solutions can be decreased by capsule exposure to a low pH value without changing the solution ionic strength.

We also explored the (TA/PVPON) coatings to determine if the permeability could be affected by direct changes in capsule suspension salt concentration. PEI(TA/PVPON)$_8$ capsules prepared at pH = 7.4 (0.01 M) were exposed to pH= 7.4 and 0.1 M NaCl for 15 min followed by the FITC diffusion measurements. Figure 5c demonstrates that increasing ionic strength from 0.01 M to 0.1 M at pH = 7.4 results in a 2-fold increase in permeability of PEI (TA/PVPON)$_8$ capsules with increase in FITC diffusion from D = (2.1 ± 0.2) 10^{-11} cm^2 s^{-1} to D = (4.4 ± 0.3) 10^{-11} cm^2 s^{-1}, respectively. Note, that the PEI(TA/PVPON)$_8$ capsules originally prepared at pH = 7.4 and 0.1 M NaCl displayed almost 1.6-fold larger permeability with D_{FITC} = (7.4 ± 0.3) 10^{-11} cm^2 s^{-1}. This implies a more compact internal arrangement of TA/PVPON layers for the condition of pH = 7.4 and low salt concentration.

Encapsulation and release of doxorubicin (DOX) in TA/PVPON capsule interiors. In order to explore the ability of the TA/PVPON multilayers to efficiently entrap DOX, the PEI(TA/PVPON)$_8$ capsules were prepared with encapsulated DOX inside the capsule interiors. Three main approaches have been reported for loading hydrophobic drugs into hollow multilayer capsules including (i) post-loading, which involves the use of hydrophobic solutions to entrap drugs, (ii) loading during the capsule assembly, i.e., assembly of multilayers on micro- or nano-crystals of poorly soluble drugs or assembly of drug molecules as the capsule shell component, and (iii) preloading, when drug molecules are first introduced inside porous templates followed by coating of the template layer-by-layer.[57,58,59] The first two methods can lead to aggregation of a capsule suspension due to use of hydrophobic oils for drug dissolution and to low encapsulation efficiencies. We applied the third approach using porous 5.3 ± 0.3 μm silica particles with surface area of 110 – 130 m^2 g^{-1} and average pore size of 24 ± 1 nm as sacrificial templates for DOX entrapment (Fig. 6a and b). Porous silica particles were incubated in DOX chloroform solution (5 mg mL^{-1}) overnight to load the drug into pores of the silica templates (Fig. 6c) followed by evaporation of chloroform from the pores for three hours under vacuum once the particles were centrifuged and separated from the solution (see Experimental section for details). The DOX-loaded particles were then encased with a PEI(TA/PVPON)$_8$ multilayer assembled at pH = 7.4 (0.01 M) (Fig. 6c). To visualize the capsule shell in confocal microscopy, Alexa Fluor 488-labeled PVPON[20] was deposited within the two last bilayers. There was no DOX present in the supernatant after the multilayer deposition was completed as confirmed with UV-vis spectroscopy. The silica cores were then dissolved using NH_4F (8M)/HF (2M) mixture at pH = 5

leaving behind DOX-encapsulated PEI(TA/PVPON)$_8$ capsules (Fig. 6c) which were dialyzed against 0.01 M phosphate buffer solution at pH = 7.4 for 2 days.

Confocal microscopy images of the DOX-encapsulated capsules shown in Figure 7 demonstrate the presence of conformal (TA/PVPON) coatings as green shells (Fig. 7a) with the capsule interiors homogeneously filled with DOX (fluorescence in Texas Red channel, Em = 613 nm) (Fig. 7b). The superimposed confocal image of the capsule walls and the capsule interiors demonstrate that all DOX is located inside the capsule cavity (Fig. 7c). This method can be also used for preparation of DOX-loaded (TA/PVPON) capsules of sub-micrometer size using porous silica particles of a ~600 nm in diameter since the micrometer solid particle formulations are as generally believed not capable of entering tumor tissues. However, in contrast to solid particle formulations, soft micrometer-sized multilayer capsules and hydrogel microparticles have been demonstrated to be taken up by the cancer cells through mechanisms different than those found for the solid nanoparticles.[52,60,61]

After capsule freeze-drying and extracting DOX, we found that 1.5 mL capsule solution (2.2×10^6 capsules/μL) contained 4.64 mg of DOX (or, 3 mg mL^{-1} DOX). This implies that 64% of DOX was efficiently loaded within the capsules with the DOX payload of 1.41×10^{-3} ng of DOX per capsule. This value is larger than that of 0.005×10^{-3} ng of DOX per capsule (as recalculated for the capsule volume) as previously shown for 1 μm thiolated poly(methacrylic acid) hydrogel capsules.[62] As suggested, concentrated dispersions of antitumor drugs of 0.5-1.0 mg mL^{-1} are required for physiologically relevant applications.[63] Apparently, the PEI(TA/PVPON)$_8$ coating allows for a highly efficient DOX loading without using lipophilic phases or surfactants to entrap DOX inside the capsules. Importantly, (TA/PVPON)$_n$ capsules are stable in high ionic strength solutions or PBS buffer as described above since their solution stabilization against aggregation is ensured by the use of hydrophilic PVPON in the non-ionic assembly with TA. Similarly, the use of highly hydrophilic block copolymers of polyaminoacids with polyethylene glycol was demonstrated to prevent colloidal aggregation during the ionic LbL assembly on ~200-nm nanoparticles.[63,64] Moreover, the hydrophilicity of PVPON has been reported to prevent protein absorption on the surfaces and affect phagocytosis of PVPON-coated polymeric particles in vitro and in vivo.[65] The percentage of PVPON-coated particles trapped in the RES organs was demonstrated to be smaller than that for the PEG-coated.[66]

We also determined the potential for DOX leakage from the capsules during time under various pH conditions. DOX-loaded capsules were exposed to 0.01 M phosphate buffer solutions at pH = 7.4, pH = 5, and pH = 10 for 24 hours and the presence of DOX in supernatants was measured using UV-vis spectroscopy. As shown in Figure 7d, the exposure of the capsules to pH = 7.4 or to pH = 5 resulted in negligible release of DOX from the capsule interiors after 24 hours with (0.96±0.01)% and (1.60±0.02)% of the released drug, respectively. Previous work showed that DOX-loaded PEO-*b*-PHEMA micelles assembled with TA into multilayers released almost 20% of the loaded DOX at pH=7.4 during the similar period of time.[35] These results demonstrate an excellent ability of the (TA/PVPON) coating to store a small molecular weight DOX within the capsule interiors for a long period of time. In contrast, (50.8±0.5)% of encapsulated DOX was found in the supernatant when the DOX-loaded PEI(TA/PVPON)$_8$ capsules were transferred to pH = 10. The capsule shells started dissolving due to TA ionization and slow capsule wall disintegration. A similar pH stability threshold has been reported previously for TA/PVPON capsules made of a shorter PVPON with M_w ~ 360000 g mol^{-1}.[29b] Although this is not a physiologically relevant pH value, it was used to confirm DOX release from the capsules. We believe this method can be used for preparation of DOX-loaded (TA/PVPON) capsules of sub-micrometer size using porous silica particles of a nanometer size since the micrometer particle formulations are generally believed not capable of entering tumor tissues. The (TA/PVPON) capsules should be capable of releasing the encapsulated drug inside the cytoplasm upon enzymatic degradation of tannic acid. This is expected to result in capsule dissolution and will be reported in our future work.[67,68]

CONCLUSIONS

In this study, we investigated differences between (TA/PVPON) coatings assembled using neutral or ionized TA, as well as from low and high salt polymer solutions for long-term encapsulation of the anticancer drug, doxorubicin (DOX). We found that the ionized state of TA in solution with high pH values lead to TA re-arrangements with quinone-like structures. The hydrogen-bonded assembly of TA with high molecular weight PVPON of M_w ~ 1,300,000 Da chemically stabilizes TA within the multilayers. We also found that TA within the TA/PVPON hydrogen-bonded complex can be deprotonated by exposing the TA/PVPON complex to a certain pH value. In this case, the degree of TA ionization is similar to that for the complex formed at the particular pH value. However, in contrast to free TA solutions, the induced TA

ionization within the TA/PVPON does not compromise the chemical stability of TA. We found that the thickness of (TA/PVPON) capsules can be regulated not only by deposition pH but also by salt concentration of the deposition solutions. Increasing deposition pH value from pH=5 to pH=7.4 leads to a 2-fold decrease in capsule thickness. However, this trend is reversed when salt concentration of the deposition solutions is increased from 0.01 M to 0.1 M NaCl. Using FRAP measurements, we have demonstrated that the permeability of (TA/PVPON) capsules prepared using low salt deposition conditions and pH=7.4 can be increased 2-fold by exposure of the capsules to 0.1 M NaCl salt solutions at the same pH. We also found that DOX can be successfully encapsulated within $(TA/PVPON)_8$ capsules prepared at pH=7.4 (0.01 M) with a high loading capacity of 1.41×10^{-3} ng of DOX per capsule and stored for a long time with a negligible DOX leakage of less than 2%.

Acknowledgement. This work was supported by NSF Award 1306110.

Experimental

Materials. Poly (N-vinylpyrrolidone) (PVPON; average M_w 1300000 g mol^{-1}), branched polyethylenimine (M_w 25000 g mol^{-1}), tannic acid (TA; M_w 1701 g mol^{-1}), hydrochloric acid, sodium hydroxide, sodium chloride, monobasic sodium phosphate, 48wt % hydrofluoric acid, and fluorescein isothiocyanate (FITC) were purchased from Sigma-Aldrich. Monodisperse nonporous silica microspheres of 4 μm in dry form were from Polysciences, Inc. Porous silica microparticles with the average diameter of 5 μm was obtained from Restek Corporation. Doxorubicin hydrochloride (DOX) was purchased from LC Laboratories. Ultrapure deionized water (0.055 μS/cm) was used (Siemens).

Formation of TA/PVPON hydrogen-bonded complexes. Monobasic sodium phosphate solution (0.01 M) with 0.1 M NaCl was used as buffer. All the experiments applied the same buffer. 100 mL TA buffer solution with concentration of 0.5 mg mL^{-1} at pH=5 was mixed with 100 mL PVPON (1 mg mL^{-1}) in the same buffer at pH=5 to form the complex. The precipitate was collected by centrifugation 30 min at 4000 rpm after mixing. The precipitate was washed 3 times with the corresponding buffer to get rid of the excess solutes. The complex prepared at pH=5 was re-dispersed in 10 mL buffer after vortex and sonication. The precipitate at pH=2, 3, 4, 5, 6, 7.4 could be maintained with the same procedure.

Fabrication of (TA/PVPON) multilayer capsules. Hollow hydrogen-bonded multilayer spherical capsules were prepared by coating 5 μm porous silica particles with $(PVPON/TA)_n$ multilayer coating followed by particle dissolution, where "n" denotes the number of bilayers. Briefly 1.5 mL of 10% silica particle suspension was pelleted in a 1.5 mL Eppendorf centrifuge tube and coated with PEI (1 mg mL^{-1} in water) as precursor. Five minutes deposition was applied followed by two times rinsing with buffer at pH=5. TA (0.5mg mL^{-1} in buffer) and PVPON (1mg mL^{-1}) were coated alternatively for 5 min with 4, 6, 8 cycles which indicated the bilayer counts. Two rinses were applied after each layer's deposition. Silica cores were dissolved in mixture of NH_4F and hydrofluoric acid to yield hollow polymeric capsules. The capsules were dialyzed against the appropriate buffer (0.01 M) for two days.

UV-Vis Spectroscopy. TA solution was prepared with the concentration of 0.5 mg mL^{-1} in 0.01 M phosphate buffer with 0.1 M NaCl. The solutions were adjusted at pH 2, 3, 4, 5, 5.5, 6, 6.5, 7, 7.4, 8, 9. UV-Vis measurements were applied within 10 min after the solutions were prepared. The complex prepared at pH=5 was re-dispersed by vortex and sonication after centrifuging in pH=5 and pH=7.4 buffer with 3 times fresh buffer rinses. The complex made at pH=7.4 was re-dispersed by vortex and sonication after centrifuging in pH=5 and pH=7.4 buffer after 3 times fresh buffer rinsing with corresponding buffers. All the UV-Vis measurements were finished within 30 min in 3.5 mL quartz cuvettes after the precipitates were formed. Both complexes and capsules were vortexed for 2 min and sonicated 10 sec with 3 times before measuring the spectra.

Ellipsometry. In-situ thickness measurements of hydrogen bonding self-assembled films were done by using a M2000U spectroscopic ellipsometer (Woollam). Before measuring, the silicon wafers were irradiated under UV light for 4 hours, washed with distilled water, and treated with concentrated sulfuric acid for 12 hours, followed by washing with distilled water and drying under compressed nitrogen. In-situ measurements were performed at 65, 70 and 75º angles in the range of 400 and 1000 nm. The ellipsometric angles were modally fitted with the silicon, silicon oxide and the films deposited on surface. All of measurements of the thickness were taken after 5 min deposition of each layer with two buffer rinses. By applying the programmable calculations with the known optical constants, the thicknesses were recorded with the Cauchy approximation. The mean squared error of the fitting data was under 50.

Atomic Force Microscopy (AFM). Atomic Force Microscopy (AFM). AFM images were collected on dry samples using DPN 5000 (NanoInk) in the close-contact mode. Tips were purchased from Agilent Technologies (resonance frequency 300 kHz, force constant 40 N/m, tip radii 10 nm). Images were analyzed using Pacific Nanotechnology Nanorule+ software (Version 2.5.05).

Confocal Microscopy (CLSM). Confocal images of PEI (TA/PVPON) capsules for DOX-encapsulated and non-encapsulated were obtained with Nikon A1R+ confocal laser microscope system equipped with 100× oil immersion objective. For the observation of capsules, a drop of capsule dispersion was placed in 8-cell Lab-Tek chambers (Electron Microscopy Sciences) followed by filling with phosphate buffer. The confocal images were obtained after the capsules settled for 3 hours. Fluorescently labeled PVPON-Alexa-488 was deposited in two last bilayers of the capsule for confocal microscopy visualization of capsules.

Fluorescence recovery after photobleaching (FRAP). The permeability experiments were performed using CLSM.[53] Briefly the fluorescence recovery of the FITC fluorescent molecules inside the capsule was recorded after photo-bleaching. Hollow capsules of PEI(TA/PVPON) with 6 and 8 bilayers were prepared as described above. 100 μL of dispersed hollow capsules solution was added into the Lab-Tek chamber glass cell with 200 μL of 1 mg mL^{-1} FITC buffer solution (0.01 M phosphate buffer with 0.1 M NaCl). The photo-bleaching experiments were performed after the capsules settle for 3 hours. Laser beam with the wavelength of 488 nm was applied within the region of interest (ROI) inside of the capsule, and pulsed at 100% intensity with 10 bleach pulse exposures of 3 ms each within the ROI. The bleaching time was ensured to completely photo-bleach FITC inside the ROI. Fluorescence recovery was recorded with 3% laser intensity by capturing 400 scans in 100 seconds. The recovery was regarded to be completed when the intensity inside the ROI became stable. ImageJ software was applied to quantify the fluorescence recovery. The recovery curve of intensity, I(t) was a function of time, t, which was fit by Origin software: $I=I_0(1-e^{-At})$, where I and I_o represented the equilibrium and initial intensity[69] and the coefficient A is a function of FITC diffusion coefficient, D. After formula derivation, we have $D=Arh/3$, where r was the radius of ROI measured using the CLSM supplied software and h was the thickness of capsular shell measured by AFM as described above.

Encapsulation of DOX. DOX-loaded capsules were prepared following the procedure described previously.[58] Specifically, 25 mg of DOX hydrochloride were mixed with 2 M equivalents of triethylamine (~30 μL), and stirred overnight in 5 mL chloroform/methanol (90/10 v/v %). The solution was filtered using 0.2 μm-syringe filter. Approximately 20 mg of porous silica particles were dispersed in 2 mL of filtered DOX solution under shaking at room temperature overnight. The DOX-loaded silica particles were centrifuged at 5000 rpm for 2 minutes, collected and dried in a vacuum oven at 40°C to evaporate chloroform, methanol and triethylamine. The dry DOX-loaded silica particles were rinsed 3 times with 0.01 M phosphate buffer and incubated in a 1 mg mL^{-1} PEI solution for 5 min followed by two buffer rinses. After that, the particles were sequentially coated with TA (0.5 mg mL^{-1}) and PVPON (1 mg mL^{-1}) using 5 min deposition time until the necessary amount of bilayers was reached. After core dissolution and dialysis in pH=7.2 (0.01 M phosphate buffer), obtained DOX-loaded capsules suspensions were stored in the dark.

Release of DOX from PEI(TA/PVPON)$_8$ capsules. The pH-triggered release of DOX from the DOX-loaded (TA/PVPON)$_8$ capsules was quantified using UV-Vis spectroscopy. The capsule concentrations were measured using a hemocytometer (Fisher Scientific). The DOX-loaded capsules were exposed to 0.01 M phosphate buffers at pH=7, pH=5, and pH=10 for certain periods of time and DOX release was measured using UV-Vis spectroscopy with the amount of released DOX quantified using the DOX calibration curve (λ_{max}=480 nm). The supernatants were separated from the capsules by centrifuging at 6000 rpm for 15 min, collected and measured in the wavelength range from 800 nm to 200 nm.

Figures

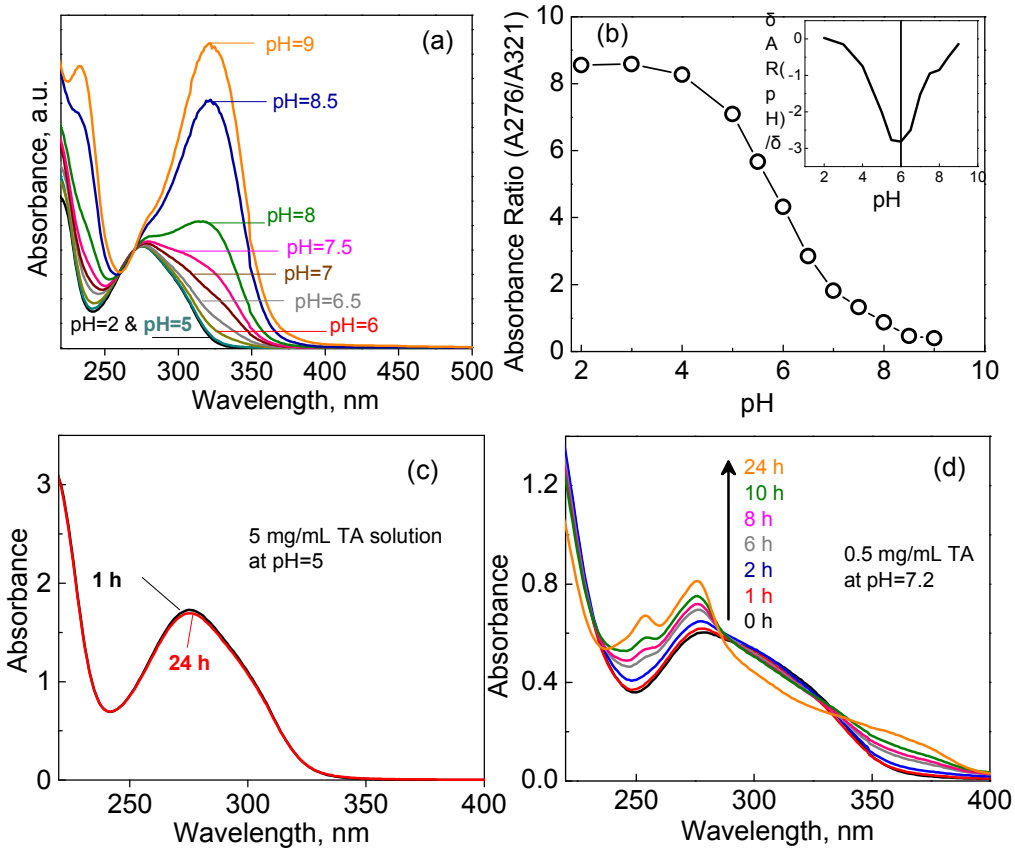

Figure 1. (a) UV-vis spectra of 0.5 mg mL^{-1} TA solutions (0.01 M phosphate, 0.15 M NaCl) at various pH values. All spectra are taken within 30 min of solution preparation. (b) The pH-dependent ratio of the absorbance at 276 nm and 321 nm. Inset shows the first-order derivative of the absorbance ratio (276 nm/321 nm)–pH curve showing the pK_a of tannic acid. (c, d) Time stability of 0.5 mg mL TA solution (0.01 M phosphate, 0.15 M NaCl) prepared at pH=5 (c) and at pH=7.4 (d).

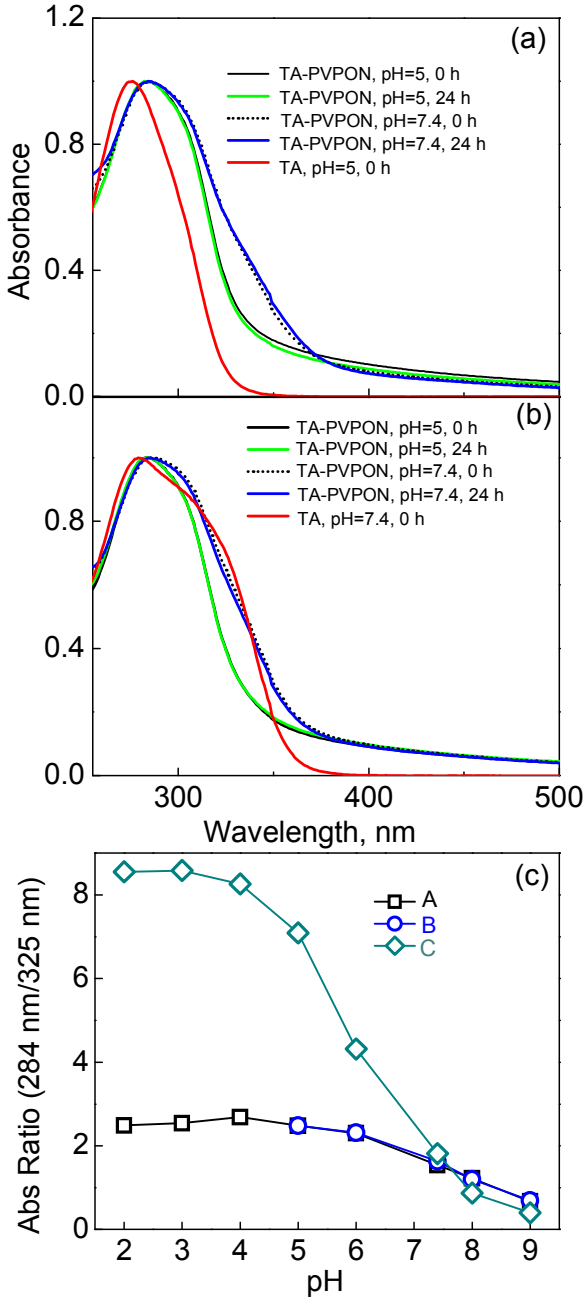

Figure 2. Time stability of TA-PVPON hydrogen-bonded complex prepared (a) at pH=5 (0.01 M phosphate, 0.15 M NaCl) and transferred to pH=7.4 and (b) at pH=7.4 and transferred to pH=5. (c) pH-Dependent ratio of absorbances at 284 nm/325 nm for TA-PVPON hydrogen-bonded complexes prepared at various pH values (0.01 M phosphate, 0.15 M NaCl) (A), for the TA-PVPON complex prepared at pH=5 and exposed to various pH values (B), and TA solutions (C).

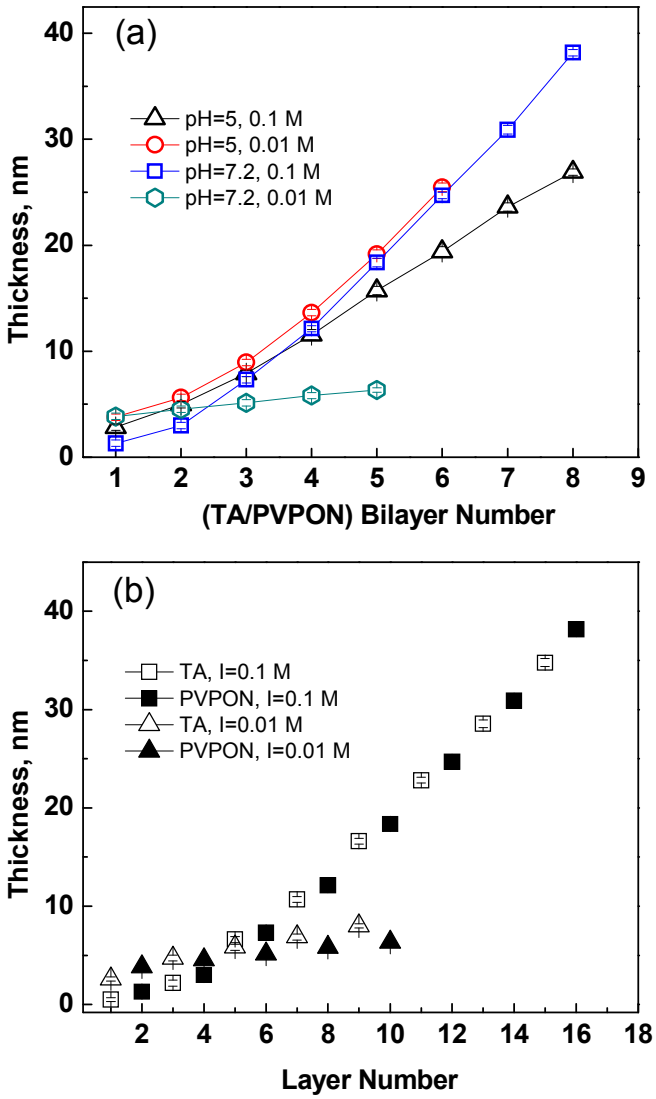

Figure 3. (a) The *in situ* growth of (TA/PVPON) bilayers at pH=5 and pH=7.4 under low (0.01 M) and high (0.1 M) ionic strength as measured by liquid ellipsometry. (b) Thickness of the TA (open symbols) and PVPON (filled symbols) layers deposited from low (triangles) or high (squares) ionic strength polymer solutions at pH=7.4.

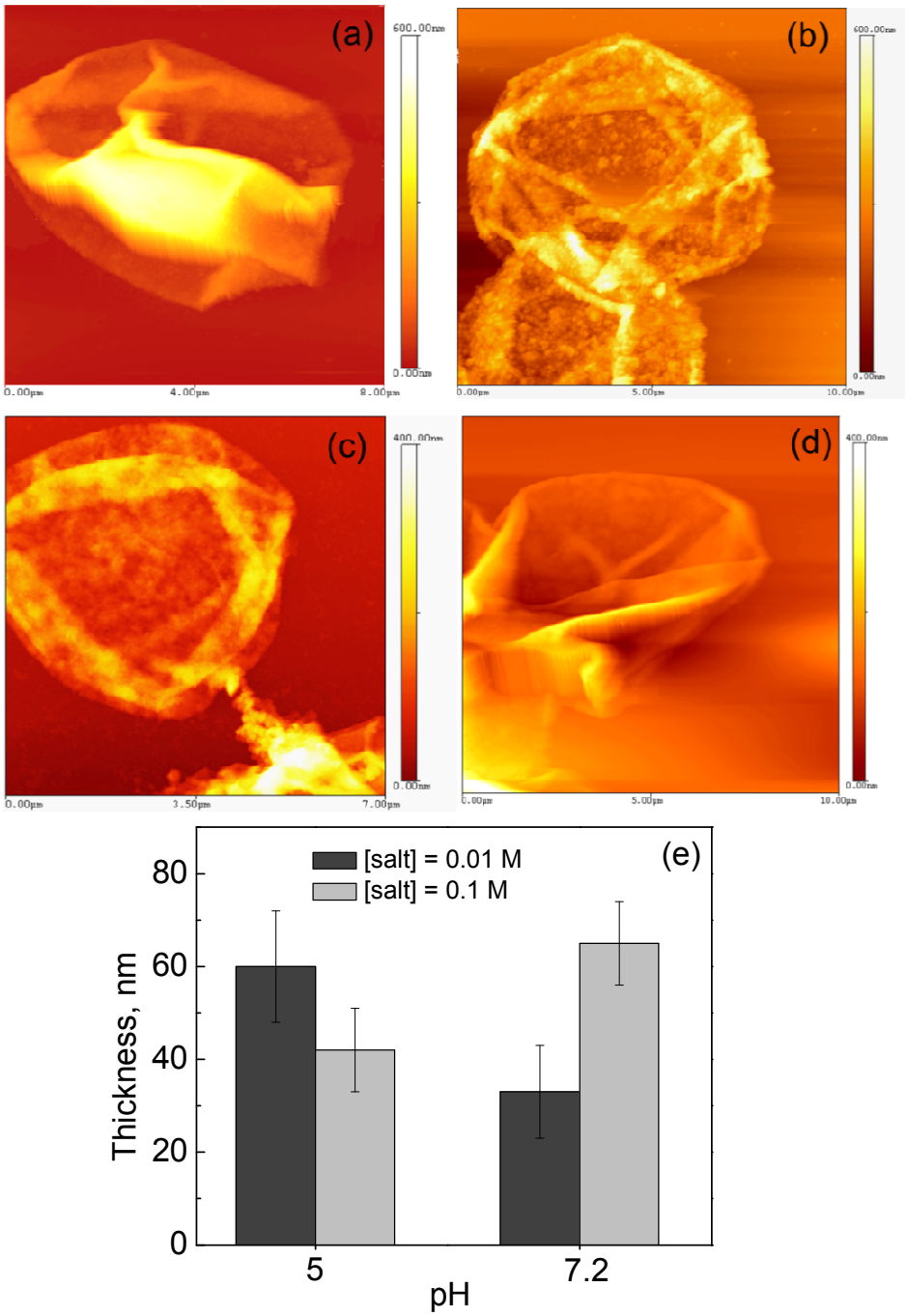

Figure 4. AFM images of PEI(TA/PVPON)$_8$ capsules assembled at pH = 5 (a, b) and at pH = 7.4 (c, d) at [salt] = 0.01 M (a, c) and [salt] = 0.1 M (b, d). Single-wall capsule thickness of the PEI(TA/PVPON)$_8$ capsules as measured using AFM.

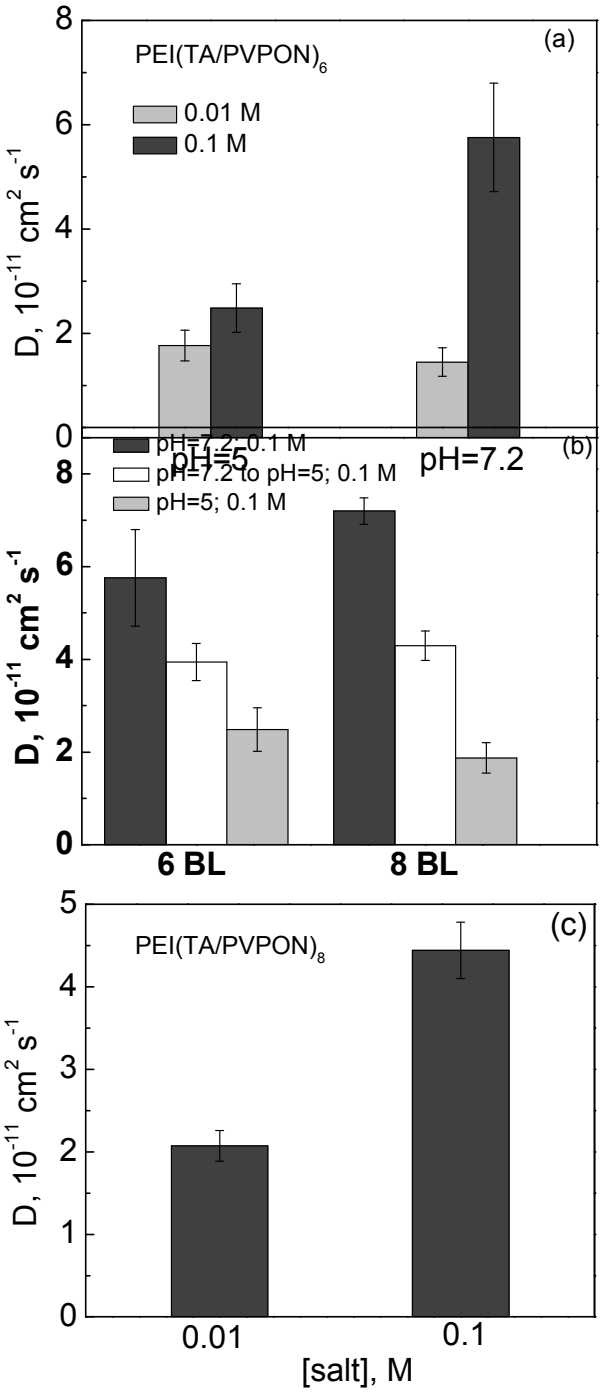

Figure 5. Diffusion coefficients for FITC molecules through $PEI(TA/PVPON)_n$ capsules with n = 6 (a, b), n = 8 (b, c) prepared at pH = 5 (a, b) or pH = 7.4 (a, b, c) at [salt] = 0.01 M (a, c) and at [salt] = 0.1 M (b)

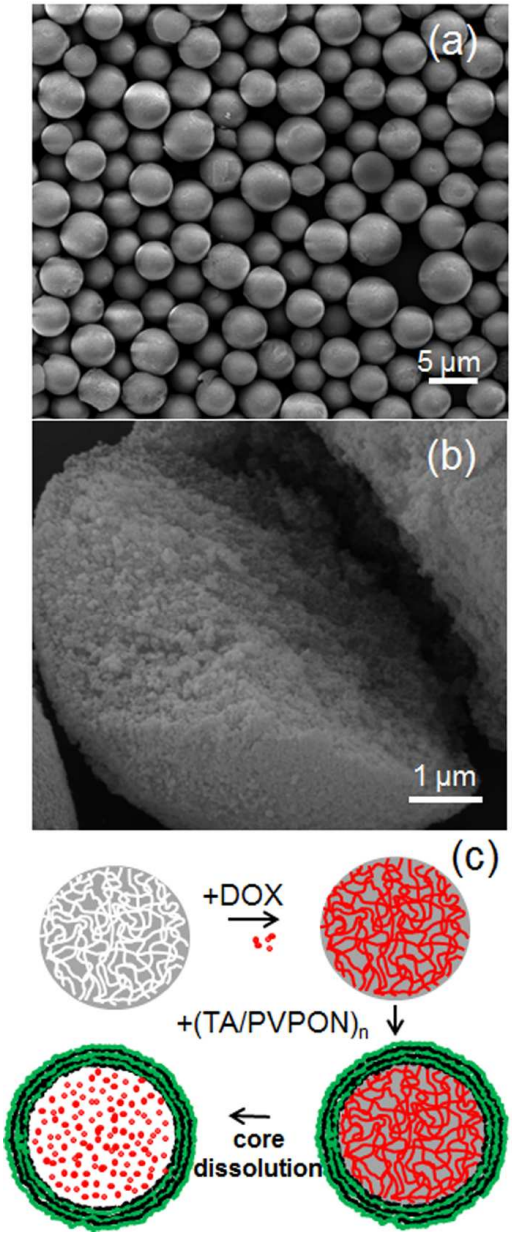

Figure 6. SEM images of 5 μm porous silica particles (a – overview; b – interiors of the porous SiO_2 particle) used for loading of DOX and encapsulating with $(TA/PVPON)_n$ multilayers as shown in (c).

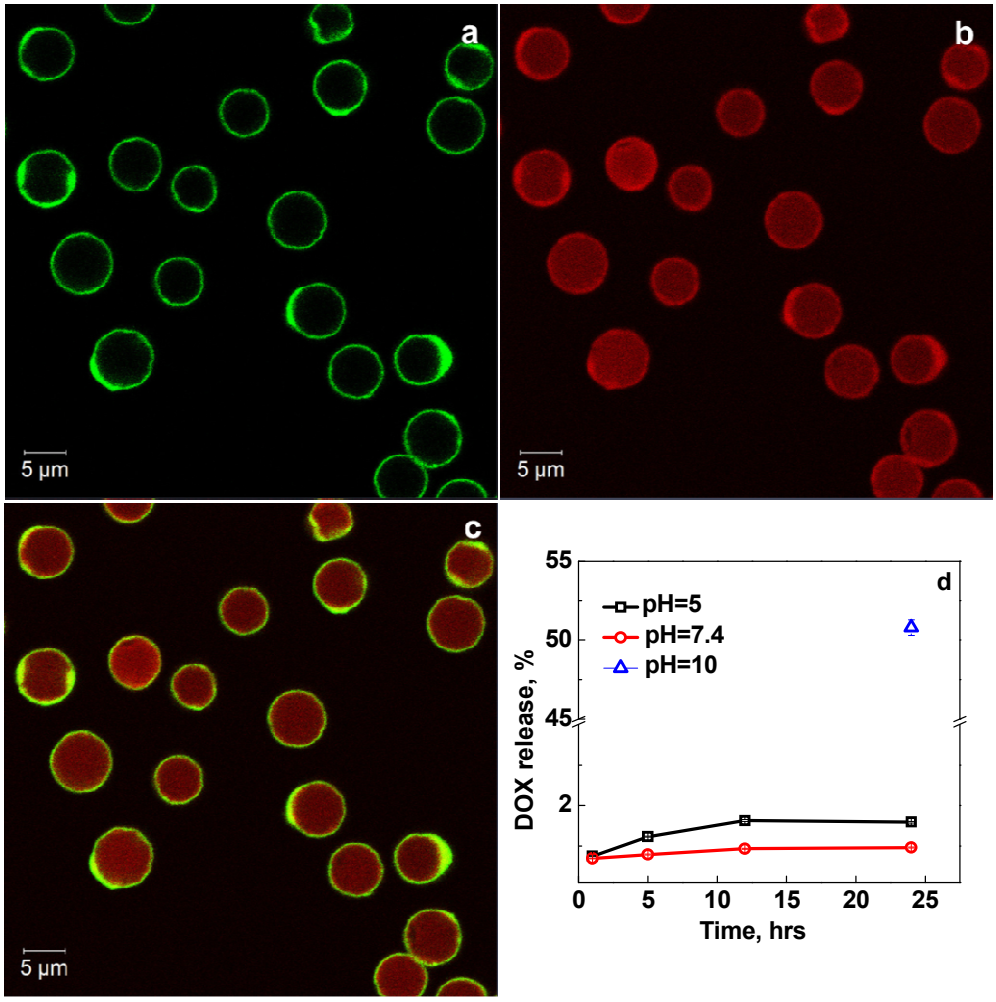

Figure 7. Confocal microscopy images of $(TA/PVPON)_8$ shells (a) with encapsulated DOX (b) and their superimposed image (c). pH-Dependent release of DOX from $PEI(TA/PVPON)_8$ capsules.

References

1 (*a*) V. P. Torchilin, *AAPS J*., 2007, **9**, E128; (*b*) E. Soussan, S. Cassel, M. Blanzat, I. Rico-Lattes, *Angew. Chem., Int. Ed.,* 2009, **48**, 274.

2 B. Thierry, *Curr. Drug. Deliv*., 2009, **6**, 391.

3 H. Cabral, N. Nishiyama, K. Kataoka, *Acc. Chem. Res*., 2011, **44**, 999.

4 W. Cao, J. Zhou, A. Mann, Y. Wang, L. Zhu, *Biomacromolecules*, 2011, **12**, 2697.

5 S. K. Riraman, B. Aryasomayajula, V. P. Torchilin, *Tissue Barriers*, 2014, **2**, e29528.

6 J. Nicolas, S. Mura, D. Brambilla, N. Mackiewicz, P. Couvreur, *Chem. Soc. Rev*., 2013, **42**, 1147.

7 A. Musyanovych, K. Landfester, *Macromol. Biosci*. 2014, **14**, 458.

8 J. Cui, M. P. van Koeverden, M. Müllner, K. Kempe, F. Caruso, *Adv. Colloid Interface Sci*., 2014, **207**, 14.

9 *Multilayer Thin Films: Sequential Assembly of Nanocomposite Materials*, ed. G. Decher and J. B. Schlenoff, John Wiley & Sons, 2012.

10 W. Tong, X. Song, C. Gao, *Chem. Soc. Rev*., 2012, **41**, 6103.

11 B. G. De Geest , N. N. Sanders , G. B. Sukhorukov , J. Demeester , S. C. De Smedt, *Chem. Soc. Rev.*, 2007 , **36** , 636.

12 (*a*) G. K. Such, A. P. R. Johnston, F. Caruso, *Chem. Soc. Rev*., 2011, **40**, 19; (*b*) T. Shutava, , M. Prouty, D. Kommireddy, Y. Lvov, *Macromolecules,* 2005, **38**, 2850; (*c*) T. Mauser, C. Dejugnat, G. B. Sukhorukov, *J. Phys. Chem. B,* 2006, **110**, 20246; (*d*) M. DeVilliers, Y. Lvov, *Adv. Drug Deliv. Rev.,* 2011, **63**, 699.

13 (*a*) V. Kozlovskaya, S. Ok, A. Sousa, M. Libera, S. A. Sukhishvili, *Macromolecules,* 2003, **36**, 8590; (*b*) J. Hiller, M. F. Rubner, *Macromolecules,* 2003, **36**, 4078; (*c*) V. Kozlovskaya, S. Yakovlev, M. Libera, S. A. Sukhishvili, *Macromolecules,* 2005, **38**, 4828; (*d*) L. L. Del Mercato, P. Rivera-Gil, A. Z. Abbasi, M. Ochs, C. Gnas, I. Zins, G. Sönnichsen, W. J. Parak, *Nanoscale,* 2010, **2**, 458.

14 (*a*) M. Matsusaki, M. Akashi, *Expert Opin. Drug Deliv.,* 2009, **6**, 1207; (*b*) W. J. Tong, C. Y. Gao, *J. Mater. Chem*., 2008, **18**, 3799; (*c*) A. G. Skirtach, A. M. Yashchenok, H. Möhwald, *Chem. Commun*., 2011, **47**, 12736.; (*d*) A. L. Becker, A. P. R. Johnston, F. Caruso, *Small,* 2010, **6**, 1836.

15 (*a*) M. M. J. Kamphuis, A. P. R. Johnston,G. K. Such, H. H. Dam, R. A. Evans, A. M. Scott, E. C. Nice, J. K. Heath, F. Caruso, *J. Am. Chem. Soc.,* 2010, **132**, 15881; (*b*) O. Shimoni, A. Postma, Y. Yan, A. M. Scott, J. K. Heath, E. C. Nice, A. N. Zelikin, F. Caruso, *ACS Nano,* 2012, ***6***, 1463.

16 K.-S. Chena, Y.-C. Hsiao, D.-Y. Kuo, M. -C. Choua, S. -C. Chud, Y.-S. Hsieh, T.-H Lin, *Leuk. Res*., 2009, **33**, 297.

17 H. Sakagami, Y. Jiang, K. Kusama, T. Atsumi, T. Ueha, M. Toguchi, I. Iwakura, K. Satoh, H. Ito, T. Hatano, T. Yoshida, *Phytomedicine*, 2000, **7**, 39.

18 K. Tikoo, M. S. Sane, C. Gupta, *Toxicol. Appl. Pharm*., 2011, **251**, 191.

19 J. P. Van Buren, W. B. Robinson, *J. Agr. Food Chem*., 1969, **17**, 772.
20 V. Kozlovskaya, O. Zavgorodnya, Y. Chen, K. Ellis, H. M. Tse, W. Cui, J. A. Thompson, E. Kharlampieva, *Adv. Funct. Mater*., 2012, **22**, 3389.
21 J. Chen, V. Kozlovskaya, A. Goins, J. Campos-Gomez, M. Saeed, E. Kharlampieva, *Biomacromolecules*, 2013, **14**, 3830.
22 M. Dierendonck, K. Fierens, R. De Rycke, L. Lybaert, S. Maji, Z. Zhang, Q. Zhang, R. Hoogenboom, B. N. Lambrecht, J. Grooten, J. P. Remon, S. De Koker, B. De Geest, *Adv. Funct. Mater*., 2014, DOI: 10.1002/adfm.201400763.
23 J. H. Park, S. H. Yang, J. Lee, E. H. Ko, D. Hong, I. S. Choi. *Adv. Mater*. 2014, **26**, 2001.
24 I. Zhuk, F. Jariwala, A. B. Attygalle, Y. Wu, M. R. Libera, S. A. Sukhishvili, *ACS Nano*, 2014, DOI: 10.1021/nn500674g.
25 Z. Gao, I. Zharov, *Chem. Mater*., 2014, **26**, 2030.
26 L. Rainville, M.-C. Dorais, D. Boudreau, *RSC Adv*., 2013, **3**, 13953.
27 K. S. Johnson, *J. Agric. Food Chem*., 2005, **53**,10120.
28 X. Zhang, M. D. Do, P. Casey, A.Sulistio, G. G. Qiao, L. Lundin, P. Lillford, S. Kosaraju, *J. Agric. Food Chem*., 2010, **58**, 6809.
29 (*a*) I. Erel-Unal, S. Sukhishvili, *Macromolecules*, 2008, **41**, 3962; (*b*) V. Kozlovskaya, E. Kharlampieva, I. Drachuk, D. Cheng, V. V. Tsukruk, *Soft Matter*, 2010, **6**, 3596.
30 E. Costa, M. Coelho, L. M. Ilharco, A. Aguiar-Ricardo, P. T. Hammond, *Macromolecules*, 2011, **44**, 612.
31 H. Ejima, J. J. Richardson, K. Liang, J. P. Best, M. P. van Koeverden, G. K. Such, J. Cui, F. Caruso, *Science*, 2013, **341**, 154.
32 A.R. Patel, J. S. ten-Hoorn, J. Hazekamp, T. B. J. Blijdenstein, K. P. Velikov, *Soft Matter*, 2013, **9**, 1428.
33 K. Driver, S. Baco, V. V. Khutoryanskiy, *Eur. Polym. J*., 2013, **49**, 4249.
34 Z. Rahman, A. S. Zidan, R. T. Berendt, M. A. Khan, *Int. J. Pharm*., 2012, **422**, 91.
35 B.-S. Kim, H. Lee, Y. Min, Z. Poon, P. T. Hammond, *Chem. Comm*., 2009, **28**, 4194.
36 A. Shukla, J. C. Fang, S. Puranam, F. R. Jensen, P. T. Hammond, *Adv. Mater*., 2012, **24**, 492.
37 Z. Zhu, N. Gao, H. Wang, S. A. Sukhishvili, *J. Controlled Release*, 2013, **171**, 73.
38 Zhu, Z.; Sukhishvili, S.A. *J. Mater. Chem*., 2012, **22**, 7667.
39 Y. Cao, W. He, *Acta Biomater*., 2013, **9**, 4558.
40 M. A. Rahim, H. Ejima, K. L. Cho, K. Kempe, M. Muellner, J. P. Best, F. Caruso, *Chem. Mater*., 2014, **26**, 1645.
41 (a) T. G. Shutava, V. E. Agabekov, Y. M. Lvov, *Russ. J. Gen. Chem*., 2007, **77**, 1494; (*b*) T. G. Shutava, S. S. Balkundi, Y. M. Lvov, *J. Colloid Interface Sci*., 2009, **330**, 276; (*c*) T. G. Shutava, M. D. Prouty, V. E. Agabekov, Y. M. Lvov, *Chem. Lett*., 2006, **35**, 1144.
42 D. Lin, N. Liu, K. Yang, Z. Zhu, Y. Xu, B. Xing, *Carbon*, 2009, **47**, 2875.
43 T. Wilke, M. Schneider, K. Kleinermanns, *Open Journal of Physical Chemistry*, 2013, **3**, 97.

44 (a) P. M. Tolstoy, B. Koeppe, G. S. Denisov, H.-H. Limbach, *Angew. Chem. Int. Ed*. 2009, **48**, 5745; (b) M. M. Kreevoy, T. M. Liang, *J. Am. Chem. Soc*., 1980, **102**, 3315.
45 E. Kharlampieva, S. A. Sukhishvili, *J. Macromol. Sci.,Polym. Rev.,* 2006, **46**, 377.
46 E. Kharlampieva, V. Kozlovskaya, S. A. Sukhishvili, *Adv. Mater*., 2009, **21**, 3053.
47 W. Tong, C. Gao, H. Möhwald, *Macromol. Rapid Commun*., 2006, **27**, 2078.
48 Z. Wang, H. Zhu, D. Li, X. Yang, *Colloids Surf. A*, 2008, **329**, 58.
49 W. Lin, Y. Guan, Y. Zhang, J. Xu, X. X. Zhu, *Soft Matter*, 2009,**5**, 860.
50 Y. Wang, A. D. Price, F. Caruso, *Mater. Chem*., 2009, **19**, 6451.
51 D. V. Volodkin, A. I. Petrov, M. Prevot, G. B. Sukhorukov, *Langmuir*, 2004, **20**, 3398.
52 V. Kozlovskaya, J. Chen, C. Tedjo, X. Liang, J. Campos-Gomez, J. Oh, M. Saeed, C. T. Lungu, E. Kharlampieva, *J. Mater. Chem. B*, 2014, **2**, 2494.
53 K. Glinel, G. B. Sukhorukov, H. Möhwald, V. Khrenov, K. Tauer, *Macromol. Chem. Phys*., 2003, **204**, 1784.
54 (a) A. A. Antipov, G. B. Sukhorukov, E. Donath, H. Möhwald, *J. Phys. Chem. B*, 2001, **105**, 2281; (b) G. Ibarz, L. Dähne, E. Donath, H. Möhwald, *Chem. Mater*., 2002, **14**, 4059.
55 G. Ibarz, L. Dähne, E. Donath, H. Möhwald, *Chem. Mater*., 2002, **14**, 4059.
56 A. Marchetti, E. Lelong, P. Cosson, *BMC Research Notes,* 2009, **2,** 7.
57 L. Hosta-Rigau , B. Städler , Y. Yan , E. C. Nice , J. K. Heath , F. Albericio , F. Caruso , *Adv. Funct. Mater*., 2010, **20**, 59.
58 Y. J. Wang, Y. Yan , J. W. Cui, L. Hosta-Rigau , J. K. Heath, E. C. Nice, F. Caruso. *Adv. Mater*. 2010, **22**, 4293.
59 (a) N. Pargaonkar, Y. Lvov, N. li, J. H. Steenekamp, M. M. de Villiers, *Pharm. Res*., 2005, **22**, 826; (b) Y. M. Lvov, P. Pattekari, X. Zhang, V. Torchilin, *Langmuir*, 2011, **27**, 1212.
60 W. Liu, X. Zhou, Z. Mao, D. Yu, B. Wang, C. Gao, *Soft Matter*, 2012, **8**, 9235.
61 A. N. Zelikin, K. Breheney, R. Robert, E. Tjipto, K. Wark, *Biomacromolecules*, 2010, **11**, 2123.
62 S. Sivakumar, V. Bansal, C. Cortez, S.-F. Chong, A. N. Zelikin, F. Caruso, *Adv. Mater*. 2009, **21**, 1820.
63 G. Parekh, P. Pattekari, C. Joshi, T. Shutava, M. DeCoster, T. Levchenko, V. Torchilin, Y. Lvov, *Int. J. Pharm*., 2014, **465**, 218.
64 T. G. Shutava, P. P. Pattekari, K. a. Arapov, V. P. Torchilin, Y. Lvov, *Soft Matter*, 2012, **8**, 9418.
65 T. E. Andersen, Y. Palarasah, M. O. Skjødt, R. Ogaki, M. Benter, M. Alei, H. J. Kolmos, C. Koch, P. Kingshott, *Biomaterials*, 2011, **32**, 4481.
66 G. Gaucher, A. Asahina, J. Wang, J. C. Leroux, *Biomacromolecules*, 2009, **10**, 408.
67 J. A. Curiel, L. Betancor, B. de las Rivas, R. Munoz, L. M. Guisan, G. Fernandez-Lorente, *J. Agric. Food Chem*., 2010, **58**, 6403.
68 H. Rodriguez, B. de las Rivas, C. Gomez-Cordoves, R. Munoz, *Food Chemistry*, 2008, **107**, 664.

69 V. Kozlovskaya, S. Harbaugh, I. Drachuk, O. Shchepelina, N. Kelley-Loughnane, M. Stone, V. V. Tsukruk, *Soft Matter*, 2011, **7**, 2364.